the detector in order to insure that one was observing a strictly dispersive process. In addition, the steady-state downstream average velocity of oxygen was always much smaller than the root mean square of the oscillation-induced velocity so that a theory for dispersion for pure oscillatory flows should be applicable. In some of our more recent experiments we filled a 5 cm diameter test section with either glass beads of 3 mm diameter or with a capillary bundle of individual radii $a = 0.047$ cm. The purpose for this was to be able to obtain measurements of D at low α. Results of most of these tests, including those reported in Ref. 1, have been recorded in Fig. 1 together with some readings on the dispersion of oxygen in soils reported by Scotter.[3] For the soil and bead results we have used the known void fraction under closely packed conditions to estimate the equivalent tube radii as $a = 0.08$ and 0.06 cm, respectively. It should be pointed out that many of the points represent more than one experimental reading which superimpose when the parameter P is used.

The experimental results are seen to reasonably approximate the theory of Watson for a $S = 0.74$ gas, indicating that one is observing a laminar dispersion process in these flows. The departure from the $P(\alpha)$ limiting curve occurring at $\alpha^2 S = \pi$ is also indicated. The scatter in the readings at large α is in part believed in part due to compressibility effects which can lead to large differences between the tidal displacements measured at the tube exit and entrance when ω is large. The observed positioning of the bead results slightly to the left of the theoretical curve suggests that the passage of gas through a collection of beads produces a better mixing than an equivalent set of tubes. Note that the frequency dependence of the dispersion coefficient at fixed S varies from frequency squared at low α to the square root of frequency at very high α. In the intermediate range $2 < \alpha < 15$, a dependence going as the first power of frequency for gases ($S = 0.74$) is a reasonable approximation. In this range the dispersion phenomenon will also be independent of the tube radius as the term a^2 in $P(\alpha)$ and α^2 will cancel.

Most recently we have the measured dispersion coefficients in branched tube systems and with a hollow cast of the canine bronchial tree. Preliminary results indicate that the dependence of D on the square of the displacement and the first power of frequency for a Womersley number range of $5 < \alpha < 12$ holds. This suggests that the process of mechanically assisted high-frequency ventilation of the pulmonary system may be in large part due to the laminar dispersion discussed above and not influenced to any large extent by secondary flow vortices existing at the bifurcations.

[1] M. J. Jaeger and U. H. Kurzweg, Phys. Fluids **26**, 1380 (1983).
[2] E. J. Watson, J. Fluid Mech. **133**, 233 (1983).
[3] D. R. Scotter, G. W. Thurtell, and P. A. C. Ratts, Soil Sci. **104**, 306 (1967).
[4] C. H. Joshi, R. D. Kamm, J. M. Drazen, and A. S. Slutsky, J. Fluid Mech. **133**, 245 (1983).
[5] G. I. Taylor, Proc. R. Soc. London, Ser. A **219**, 186 (1953).
[6] H. Schlichting, *Boundary Layer Theory* (McGraw-Hill, New York, 1968), p. 419.
[7] U. H. Kurzweg, J. Heat Transfer (to be published).
[8] G. W. Howell, MS thesis, University of Florida, 1984.

On the scaling of the turbulence energy dissipation rate

K. R. Sreenivasan
Mason Laboratory, Yale University, New Haven, Connecticut 06520

(Received 29 November 1983; accepted 23 February 1984)

From an examination of all data to date on the dissipation of turbulent energy in grid turbulence, it is concluded that, for square-mesh configuration, the ratio of the time scale characteristic of dissipation rate to that characteristic of energy-containing eddies is a constant independent of Reynolds number, for microscale Reynolds numbers in excess of about 50. Insufficient data available for other grid configurations suggest a possibility that the ratio could assume different numerical values for different configurations. This persistent effect of initial conditions on the time scale ratio is further illustrated by reference to the jet-grid data of Gad-el-Hak and Corrsin.

It has long been believed, essentially on dimensional grounds, that the time scale of the energy dissipation rate ϵ in fully turbulent flows is of the same order of magnitude as the characteristic time scale of the energy containing eddies (except where the effects of viscosity are directly felt, such as near a smooth wall). Probably the only *direct* attempt to test this notion against experiments has been that due to Batchelor,[1] who plotted the quantity $\epsilon L_f / u^3$ (where L_f is the longi-

0031-9171/84/051048-04$01.90

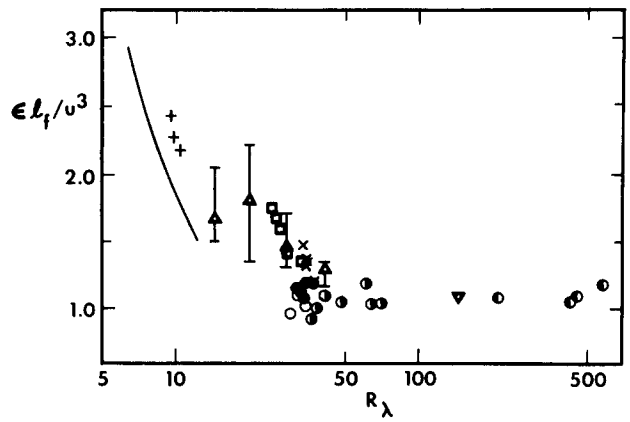

FIG. 1. The quantity $\epsilon L_f/u^3$ for biplane square-mesh grids. All data except + are for the initial period of delay, and are explained in Table I. + indicate typical data[13] in the final period of decay. — corresponds to Eq. (1).

tudinal integral scale, and u is the root-mean-square longitudinal velocity fluctuation) against the distance from the grid. He concluded that, in the so-called initial period of decay, the data are not generally inconsistent with the above expectation. (Here, u^2/ϵ can be regarded as the time scale of dissipation, and L_f/u as that characteristic of large eddies. While this latter quantity is not directly related to the time scale of the energy-containing eddies, the difference is not sufficiently significant to mask a real trend if it exists.) However, the relatively large scatter in the data collected by Batchelor permits one to speculate a weak Reynolds number dependence at least in the relatively narrow range covered ($14.4 \leqslant R_\lambda \leqslant 41$, where R_λ is the microscale Reynolds number based on u, the Taylor microscale λ, and kinematic viscosity ν). For example, Saffman[2] has pointed out that a logarithmic or $-\frac{1}{4}$ power dependence of $\epsilon L_f/u^3$ on R_λ is not necessarily inconsistent with the data. The point at issue is important, and is indeed one of the few key elements of a "semirational turbulence theory," and so, it seems desirable to examine the question in the light of much more recent data that have become available, extending over a wide Reynolds number range and a variety of conditions. This is the main purpose of this letter. We confine ourselves to data in grid turbulence (although we have examined shear flows also) (see Table I). With one exception (which will be noted), only those experiments in which L_f was either explicitly supplied by the authors,[3–12] or could be evaluated by us via their measured correlation function of spectral density, have been considered.

For consistency, we define $\epsilon = -\frac{3}{2} U_0(du^2/dx)$, with U_0 as the mean velocity in the test-section, even when, occasionally, one or both of the remaining two fluctuation components were measured; du^2/dx was evaluated from the best power fit possible for the u^2 data in the initial period of decay. (On those occasions where the authors gave a ready number for ϵ, we have always cross-checked it with the original data.)

Figure 1 shows all the data for biplane, square-mesh grids. It is clear that $\epsilon L_f/u^3$ is sensibly independent of R_λ for $R_\lambda \gtrsim 50$ although, for lower R_λ, there seems to be a recognizable trend.

That $\epsilon L_f/u^3$ could depend on R_λ for small R_λ is not surprising, considering that the constancy of $\epsilon L_f/u^3$ is only an asymptotic expectation. In particular, at very low Reynolds numbers where the inertia forces are weak, such as in the final period of decay, it is easily shown that

$$\epsilon L_f/u^3 = (\pi/2)^{1/2}(15/R_\lambda), \tag{1}$$

if we recall the relation $\epsilon = 15\nu u^2/\lambda^2$ and the result[1] that $L_f/\lambda \approx (\pi/2)^{1/2}$. Typical experimental data from Bennett and Corrsin,[13] shown in Fig. 1, deviate from Eq. (1) because the measured values of L_f/λ are higher than $(\pi/2)^{1/2}$ and increase weakly as the Reynolds number decreases.

It is pertinent here to make reference to Rotta's[14] work. Rotta assumed that the spectral energy transfer occurs according to Heisenberg's theory,[15] and further that the so-called Loitsianskii invariant (see, for example, Ref. 1, p. 92) exists and is numerically equal to 4. With these assumptions he calculated that $\epsilon L_f/u^3 \to 0.76$ as $R_\lambda \to \infty$. (The corresponding value from Fig. 1 is around 1.) He also smoothly interpolated between this high Reynolds number solution and the low Reynolds number solution given by Eq. (1). The interpolated curve shows a behavior qualitatively not unlike that of the data in Fig. 1. However, because of the various dubious assumptions involved in the calculations, and also because of the numerical disparity in the high Reynolds number limit mentioned earlier, it was thought unnecessary to reproduce Rotta's interpolation curve.

While the situation appears quite satisfactory with respect to square-mesh grids, it is not so clear for other types of grids. For example, the quantity $\epsilon L_f/u^3$ for the flow behind an array of parallel rods,[16,17] plotted in Fig. 2, shows a considerable scatter and, more importantly, is higher on the average (assuming that the average is meaningful) than the corresponding square-mesh value. (It may be argued that the turbulence behind an array of parallel rods may not have attained homogeneity and isotropy to the same degree of approximation as in the case of square-mesh grids. We may,

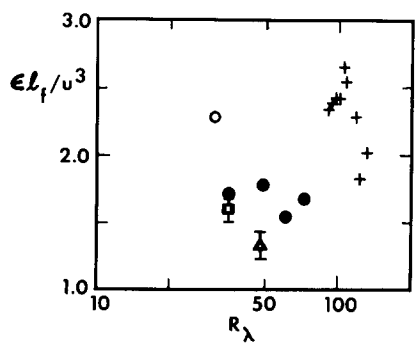

FIG. 2. $\epsilon L_f/u^3$ for grids of parallel rods and a slats grid. Parallel rods: △, $M = 2.54$ cm. $\sigma = 0.37$, $x/M = 60$ (Ref. 16); +, $M = 10.2$ cm, $\sigma = 0.37$, $30 \leqslant x/M \leqslant 70$ (Ref. 17); 0, $M = 2.54$ cm, $\sigma = 0.31$; ●, $M = 2.54$ cm; $\sigma = 0.37$. The last two are at $x/M = 50$ from Ref. 18. □, slats grid, $M = 1.9$ cm, $\sigma = 0.21$, $x/M = 47$ from Ref. 16.

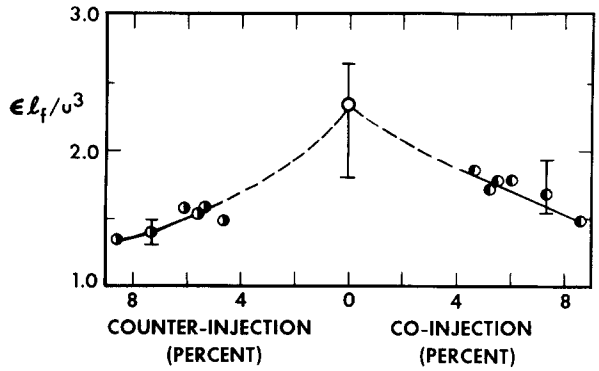

FIG. 3. $\epsilon L_f/u^3$ for jet-grids of Ref. 17. 0 at zero injection rate is an average of 10 data points ($99 \leqslant R_\lambda \leqslant 130$). Both ◐ and ◑ at injection rates of 7.32% are averages of six points each. $R_\lambda \approx 110$ for ◐ and 150 for ◑.

however, note that in the region of measurement in Ref. 17, simple measures of homogeneity, such as the uniformity of mean velocity distribution in the "core region" of the wind tunnel and of isotropy such as the ratios of the root-mean-square intensities in different directions, were found to be rather typical.) Also plotted in Fig. 2 is a point for a slats grid (looking like an open Venetian blind) from Ref. 16. In Fig. 2, the length scale L_f for Gad-el-Hak and Corrsin's[17] measurements was obtained from the authors' tables, while for the Stewart and Townsend data[16] it was computed by the area L_g under transverse correlation curves and the assumption that $L_f = 2L_g$. (The vertical bar corresponds to the extremes on L_f depending upon which of the transverse correlation functions was used for integration.) Harris[18] did not measure L_f, and this is the exception mentioned earlier. For the typical data of Harris we have used, L_f/M was taken from Ref. 17 with the hope that the essentially similar configuration, grid solidity, and experimental conditions justify this step.

TABLE I. Guide to the biplane grid data of Fig. 1.

Source	Grid type	x/M	Symbol
Corrsin[3]	Biplane, round rods $M = 1.27$ cm, 2.54 cm $\sigma = 0.44$	34–230	□
Batchelor and Townsend[4]	Biplane, round rods $\sigma = 0.34$, $M = 0.635$, 1.27 and 2.54 cm	20–180	△[a]
Baines and Peterson[5]	Biplane, square rods $M = 3.38$ cm, $\sigma = 0.44$[b]	27–64	—
Mills *et al.*[7]	Biplane, round rods $M = 2.54$ cm, $\sigma = 0.44$	17–65	○
Kistler and Vrebalovich[8]	Biplane, square rods, $M = 17.15$ cm, $\sigma = 0.34$	45	◐
Comte-Bellot and Corrsin[9]	Biplane, square rods $M = 2.54$ and 5.08 cm $\sigma = 0.34$	42–385	◑
Lin and Lin[10]		55	▽[c]
Yeh and Van Atta[11]	Biplane, round rods $M = 4$ cm, $\sigma = 0.36$	23–48	×
Sreenivasan *et al.*[12] (only typical data presented)	Biplane, round rods $M = 2.54$ cm, $\sigma = 0.44$	12–102	●

[a] The symbol △ actually represents the mean of several sets of data whose range is indicated in Fig. 1 by a vertical bar in each case. At $R_\lambda = 14.4$ there are 9 sets of data, 15 at $R_\lambda = 20.3$, 9 at $R_\lambda = 28.4$, and 3 at $R_\lambda = 41$.

[b] Baines and Peterson's data cover seven biplane grids. Three grids have solidity of 0.61, 0.75, and 0.89, and are likely to have produced unstable flow downstream.[6] In two other cases ($M = 30.5$ cm and 20.3 cm), measurements did not proceed beyond x/M of about 12.5. In the seventh case, which alone could be considered here, $\epsilon L_f/u^3$ ranges from 1.29 to 1.86; unfortunately, the corresponding Reynolds numbers are unknown, preventing us from plotting the data in Fig. 1.

[c] Lin and Lin's grid is unconventional in that it is a complex structure of heated elements repeatedly folded into compact flow channels, which themselves are arranged in a square-mesh fasion. Its exclusion from Fig. 1 does not at all affect the conclusions.

The data of Figs. 1 and 2 allow us to speculate that $\epsilon L_f/u^3$ may take on different values for different grid configurations. (Unfortunately, the perforated disc data of neither Ref. 5 nor Ref. 19 could be included because L_f is not available.) Investigators who compare theories of isotropic turbulence with grid turbulence data often implicitly assume that the turbulence sufficiently far behind a grid attains a character independent of the configuration of the grid. It does not quite appear justified, presumably because the scales of turbulence strongly affected by grid geometry contain a significant fraction of energy. This dependence on initial conditions can be seen more directly by examining the data of Gad-el-Hak and Corrsin,[17] who used an array of parallel rods, in combination with several jets of fluid (coflowing as well as counterflowing) evenly distributed along each rod, to produce nearly homogeneous and isotropic turbulence. Figure 3 shows that $\epsilon L_f/u^3$ in the downstream region correlates reasonably well with the injection rate of the jets. It is worth noting that for large injection rates, $\epsilon L_f/u^3$ seems to approach a value appropriate to square-mesh grid. This seems quite reasonable physically because the grid is essentially a parallel-rod type for small jet speeds, but becomes more square-mesh type at high jet speeds.

If it is true that the effects of grid geometry do persist, it is legitimate to ask why there does not seem to be any noticeable difference (see Fig. 1 and Table I) between square-mesh grids of round rods and square-mesh grids of square rods. One would also like to know, for instance, whether there are noticeable differences in $\epsilon L_f/u^3$ between single plane grids of square rods and single plane grids of round rods. We suspect that the asymptotic character of two grid flows will not be "noticeably" different if the grid configurations are "sufficiently" close, and that, even in square-mesh grids, if one changes the grid solidity σ by a large amount, the flow characteristics will change significantly. We note (with some surprise) that a large body of literature on turbulence behind square-mesh grids is confined to grids of solidity not very different from 0.4 (see Table I).

ACKNOWLEDGMENT

During the preparation of this letter the author held a Humboldt fellowship. Thanks are due to Dr. H. Oertel for the hospitality extended at his institute in DFVLR, Göttin-

gen, and Dr. L. Kleiser for bringing Rotta's work to his attention.

This work forms a part of inquiry into the effects of initial conditions on the development of turbulent flows, supported by the Air Force Office of Scientific Research.

[1]G. K. Batchelor, *The Theory of Homogeneous Turbulence* (Cambridge U. P., Cambridge, 1953), Chap. 6.
[2]P. G. Saffman, in *Topics in Nonlinear Physics*, edited by N. Zabusky (Springer, Berlin, 1968).
[3]S Corrsin, Ae.E. thesis, California Institute of Technology, 1942.
[4]G. K. Batchelor and A. A. Townsend, Proc. R. Soc. London Ser. A **193**, 539 (1948).
[5]W. D. Baines and E. G. Peterson, Trans. Am. Soc. Mech. Eng. **73**, 477 (1951).
[6]S. Corrsin, in *Hanbuch der Physik*, edited by S. Flugge and C. Truesdell (Springer, Berlin, 1963), Vol. 8, Part 2, p. 524.
[7]R. R. Mills, A. L. Kistler, V. O'Brien, and S. Corrsin, N.A.C.A. Technical Note No. 4288, 1958.
[8]A. L. Kistler and T. Vrebalovich, J. Fluid Mech. **26**, 37 (1966).
[9]G. Comte-Bellot and S. Corrsin, J. Fluid Mech. **48**, 273 (1971).
[10]S. C. Lin and S. C. Lin, Phys. Fluids **16**, 1587 (1973).
[11]T. T. Yeh and C. W. Van Atta, J. Fluid Mech. **58**, 233 (1973).
[12]K. R. Sreenivasan, S. Tavoularis, R. Henry, and S. Corrsin, J. Fluid Mech. **100**, 597 (1980).
[13]J. C. Bennet and S. Corrsin, Phys. Fluids **21**, 2129 (1978).
[14]J. C. Rotta, *Turbulente Strömungen* (Teubner, Stuttgart, 1972), p. 116.
[15]W. Heisenberg, Z. Phys. **124**, 628 (1948).
[16]R. W. Stewart and A. A. Townsend, Philos. Trans. R. Soc. London Ser. A **243**, 359 (1951).
[17]M. Gad-el-Hak and S. Corrsin, J. Fluid Mech. **62**, 115 (1974).
[18]V. G. Harris, M. S. thesis, Johns Hopkins University, 1965.
[19]G. Comte-Bellot and S. Corrsin, J. Fluid Mech. **25** 657 (1966).

Parametric excitation of ion Bernstein waves by a fast wave antenna in the ion cyclotron frequency range

F. Skiff, M. Ono, and K. L. Wong
Plasma Physics Laboratory, Princeton University, Princeton, New Jersey 08544

(Received 27 December 1983; accepted 22 February 1984)

Parametric excitation of ion Bernstein waves is observed with an ICRF fast wave induction loop antenna in the ion cyclotron frequency range ($\omega_0 \sim 2\Omega_i - 4\Omega_i$). Important features of the decay process are investigated and discussed.

Fast wave heating in the ion cyclotron frequency range is one of the most promising schemes for heating fusion plasmas to ignition temperatures. As the input power and consequent rf energy levels employed in plasma heating increase, it will become increasingly important to understand the detailed physics of the heating process. For example, to answer the important questions of where and how rf energy is deposited in a plasma requires the consideration of both linear and nonlinear processes.

In this letter we present the first experimental verification of a decay instability in which an ion Bernstein wave (IBW) and an ion quasimode (IQM) are parametrically excited by the near-field electric field of an ICRF antenna. Onset of this decay is observed with a low-threshold electric field in a warm-ion hydrogen plasma over a wide range of parameters. Since the IBW propagates for $\omega \leqslant \omega_{pi}$, the decay is allowed in high density regions and essentially complements the parameter space of the previously reported decay into electron plasma waves (EPW) and ion quasimodes.[1] Decay into ion Bernstein waves may have an important effect on the deposition of rf energy during second-harmonic (or higher) fast-wave heating where the waves are launched from the low-field side with $\omega_0 > 2\Omega_i$.

In the context of uniform-pump theory the magnetosonic fast waves and the IBW can be parametrically coupled (with the fast wave acting as pump) when the relative particle drift excursions in the pump field divided by the decay wave wavelength exceed a threshold value. This threshold is determined by the linear damping of the IBW. In the ion cyclotron frequency range the ion and electron drift excursions (in the $\mathbf{E}\times\mathbf{B}$ direction) are comparable and oppositely directed. Ion motion, therefore, can enhance parametric coupling in this frequency range.[1] The parametric dispersion relation relevant to our experiment can be written[2]

$$\gamma = -\gamma_2 + \sum_{\sigma,\eta} \frac{|\mu_\sigma - \mu_\eta|}{8|\partial\epsilon/\partial\omega_2|} \operatorname{Im} \frac{\chi_\sigma(\omega_1)\chi_\eta(\omega_1)}{\epsilon(\omega_1)},$$

with

$$\mu_\sigma = \left(\frac{q}{m}\right)_\sigma \left[\left(\frac{E_{0\parallel} k_\parallel}{\omega_0^2} + \frac{\mathbf{E}_{0\perp}\cdot\mathbf{k}_\perp}{\omega_0^2 - \Omega_\sigma^2}\right)^2 + \frac{(\mathbf{E}_{0\perp}\times\mathbf{k}_\perp\cdot\hat{z})^2\Omega_\sigma^2}{(\omega_0^2 - \Omega_\sigma^2)^2\omega_0^2}\right]^{1/2}, \quad (1)$$

where μ_0 is the ratio of drift excursion of species σ in the pump field $\mathbf{E}_0$ to the decay wave wavelength $2\pi/k$, and $\epsilon = \mathbf{I} + \Sigma_\sigma \chi_\sigma$ is the hot plasma dielectric response, $\epsilon = \hat{k}\cdot\epsilon\cdot\hat{k}$, $\chi_\sigma = \hat{k}\cdot\chi_\sigma\cdot\hat{k}$, $\hat{k} = \mathbf{k}/k$, and χ_σ is the contribution to the plasma susceptibility of σ-type particles. The subscripts σ, η refer to all particle species, and the subscripts 0,

 0031-9171/84/051051-04$01.90